Robotica: (2023) volume 41, pp. 16–30. © The Author(s), 2020. Published by Cambridge University Press.
doi:10.1017/S0263574720001174

Optimal Architecture Planning of Modules for Reconfigurable Manipulators

Anubhav Dogra*, Srikant Sekhar Padhee and Ekta Singla

Department of Mechanical Engineering, Indian Institute of Technology Ropar, Rupnagar, Punjab 140001, India
E-mails: sspadhee@iitrpr.ac.in, ekta@iitrpr.ac.in

(Accepted November 21, 2020. First published online: 18 December 2020)

SUMMARY
Modules are requisite for the realization of modular reconfigurable manipulators. The design of modules in literature mainly revolves around geometric aspects and features such as lengths, connectivity and adaptivity. Optimizing and designing the modules based on dynamic performance is considered as a challenge here. The present paper introduces an Architecture-Prominent-Sectioning (*APS*) strategy for the planning of architecture of modules such that a reconfigurable manipulator possesses minimal joint torques during its operations. Proposed here is the transferring of complete structure into an equivalent system, perform optimization and map the resulting arrangement into possible architecture. The strategy has been applied on a set of modular configurations considering three-primitive-paths. The possibility of getting advanced/complex shapes is also discussed to incorporate the idea of a modular library.

KEYWORDS: Modules; Reconfigurable; Serial manipulator; Architecture design; Optimization.

1. Introduction

Reconfigurable manipulators are the next generation robotic tools as they promise the deliverance of high flexibility, adaptability and customization.[1] Standard configuration robotic manipulators had been in regular use to perform a large set of tasks. However, when a manipulator is required to do a specific task in a cluttered environment, which may be *non-repetitive* in nature, a given conventional robotic arm may not be useful.[2] In such cases, a robot with adaptive attributes would be more helpful. *Modular reconfigurable manipulators* have gained attention for such applications. Reconfiguration is achieved if the manipulators' geometric and inertial parameters can be altered such as if the system has inherent reconfigurable mechanisms[3] or with the use of modular elements.[4] Modules are designed so as to be adaptable to designed parameters, say the Denavit–Hartenberg (DH) parameters and can be assembled in series according to certain assembly rules so that geometric parameters can be altered in the modules itself to get a new configuration.[5] Major challenge to accomplish this concept lies in how to design an optimal architecture of the adaptive module to facilitate advanced robot designs and applications so that, a modular library be developed, to accomplish a wide variety of tasks in varied environments?

Reconfiguration and modularity have received attention of researchers from last two decades in various areas viz. mobile robots, long serial chains, industrial manipulators and so forth.[6] Reconfiguration using modular designs has gained much popularity. Modules are sometimes

* Corresponding author. E-mail: 2016mez0019@iitrpr.ac.in

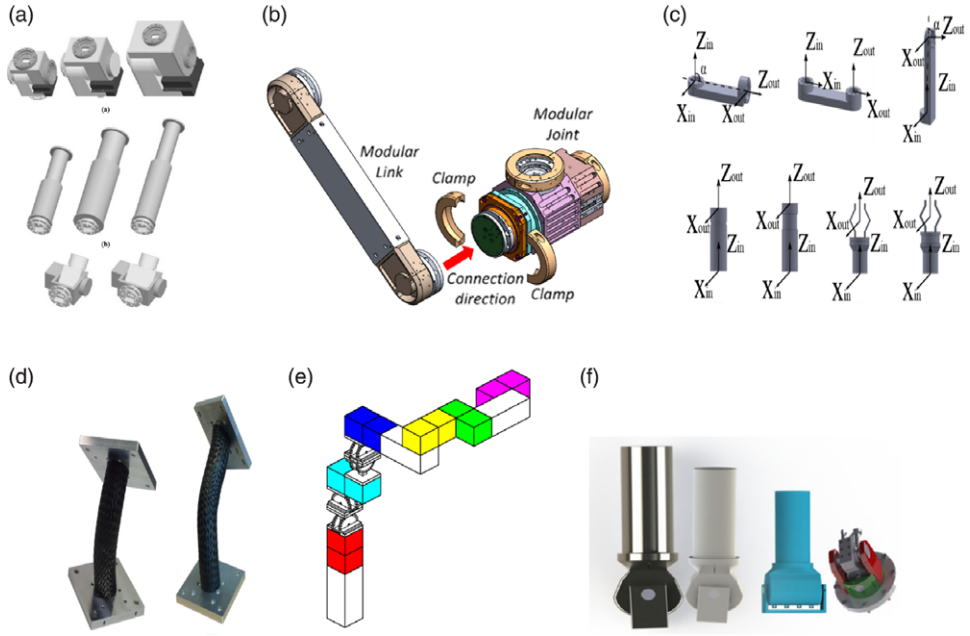

Fig. 1. Modules for reconfigurable manipulators: (a), (b) and (c) Joint modules and link modules designs for standard configurations. (d), (e) and (f) Modular designs which can also incorporate unconventional robotic parameters.

classified as link modules or passive modules, active or joint modules, and other add-on modules such as base modules and end-effector modules.[7] Modular components normally consist of link and joint modules with fixed lengths, assembled in parallel or perpendicular configurations to achieve twist angle as 0° or 90°.[8,9] Further flexibility is sometimes achieved using variable length modules[10] as shown in Fig. 1(a), and including unconventional parameters.[2,11,12] Here, the unconventional parameters focus on the twist angles of the joints other than 0° or 90°. Modules in Fig. 1(d), (e), (f) are the examples of such modular approaches discussed in few recent studies. Gaps have been observed in the information related to arrangement of these components, that is, the modular architecture. Less discussions are found in literature to support the selected architecture and that leads to possibilities of improving both the design and connectivity of the modular architecture. Normally, achieving optimal kinematic performances[13] of the manipulators sets a way to decide the required configuration of the robotic manipulator[14] and accordingly modules are planned to achieve that required twist angles and offsets if any. Only in a few cases, kinetostatic and dynamic performances are considered to decide the configurations.[15–17] Focus here is at the architecture planning of the modules for an optimal dynamic performance. Since the inertial parameters do change while reconfiguration of a modular assembly – due to the variation in number of modules, changing variants in modules or frame to frame distance using extensions, etc. – it is worthwhile to focus on fundamental architecture of the modules itself. Therefore, it is important to identify the significant components in modules which are affecting the dynamic performances and to optimize the architecture of the modules. This rearrangement in the modular architecture is not supposed to be changed for any task, as it is designed for dynamic performance over a set of primitive trajectories.

This paper is organized as follows. Section 2 defines the problem and motivation for the work and briefs about the design strategy for the modules. Section 3 defines optimization problem formulation which includes optimization model and objective function computation. Section 4 shows the results considering three primitive paths for a modular configuration followed by discussions regarding current and future works, with the conclusion in the last section.

2. Motivation and Problem Definition

Motivation of this work arrives from the authors' work in modules. The modules had been critically designed keeping in consideration the geometrical and the kinematic aspects like the minimum length of the modules, transmission elements for the joint-rotation and the twist angle adjustments.[2] This paper focuses on the optimal architectural planning of the modules. Few works have been

https://doi.org/10.1017/S0263574720001174 Published online by Cambridge University Press

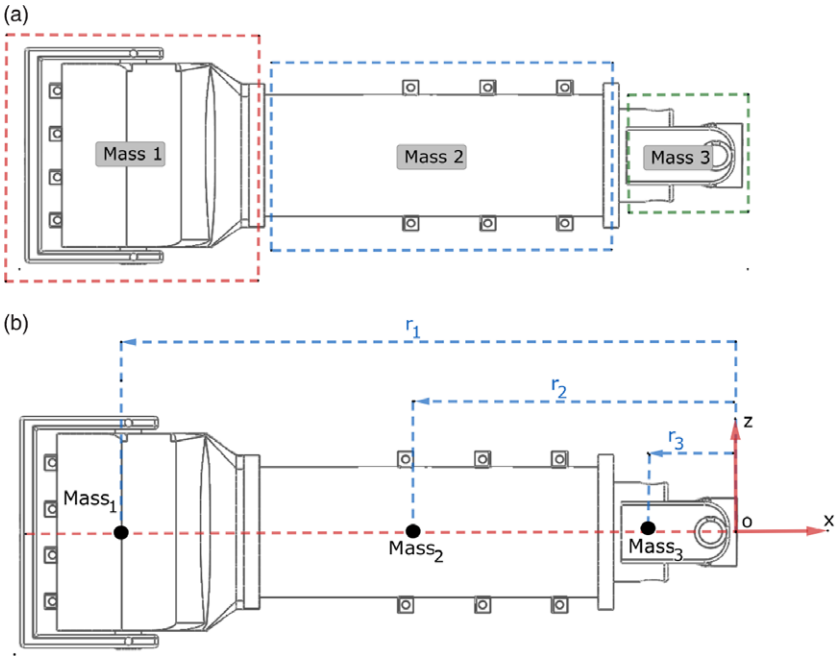

Fig. 2. Architecture-Prominent-Sectioning (APS) of a module. (a) Three prominent sections of the module are identified and (b) Centre of masses (CoMs) of three sections is taken as equivalent point mass parameters.

seen in this area focusing on the dynamic balancing of a mechanism for specific manipulator configurations.[18–21] Novelty of this paper is the optimization of the modular architecture with respect to dynamic torques, which are basic building blocks and used to assemble any n-degrees of freedom (DoF) serial manipulator configuration. The proposed methodology of Architectural Prominent Strategy (APS) for sectioning the original architecture, utilization of equimomental system with three types of primitive trajectories for analysing the dynamic performance in a general domain and applicability of the strategy for not just a specific configuration but general in nature are the major contributions in the field. The results may strongly be connected to the advanced techniques of 3D printing for non-uniform material requirements.

The problem is defined as – given the geometrical and inertial parameters of modular components, which are kinematically designed to build any customized modular configuration for prescribed *DH* parameters – how to alter the architectural arrangement of the modular components so that the architectural design is dynamically optimal. For the modules to be utilized for assembling several different configurations and for different tasks, the optimization be validated for a larger domain with a larger set of trajectories. Proposed here is the transferring of the architecture of the modules and hence the manipulator into an equivalent system, perform optimization and map the resulting arrangement into possible architecture.

3. Methodology

An architecture of a module may include various elements such as transmission elements, stiffness elements and actuators. Significant elements in a module need to be identified and accordingly, its mass parameters $[m_1, m_2, m_3, ..., m_j]$ and location parameters $[x_1, y_1, z_1, x_2, y_2, z_2, ..., x_j, y_j, z_j]$ can be the possible design variables. However, such an option is not recommendable for two reasons. First, these inertial features are depending upon each other for a rigid body and tinkering the design variables during optimization is not straight forward. Secondly, to introduce creativity it is desirable not to focus only on visible parameters. Towards that, an *APS* strategy is introduced. *APS* consists of sectioning the repeatable architecture into prominent sections, as shown in Fig. 2. Each section could consist of internal elements such as transmission elements which are motor, gears, shafts, etc. and stiffness elements which are the casings.[22]

To formulate and implement *APS* for optimizing dynamic performance, a systematic approach would be required, majorly focusing on trajectory to be followed and constraints on the design variables. Objective here is to get an optimal architecture of these adaptive modules such that the

https://doi.org/10.1017/S0263574720001174 Published online by Cambridge University Press

reconfigurable manipulators assembled out of these possess minimal joint torques. In this regard, some assumptions have been considered while formulating the strategy as below.

1. Link lengths are not considered as design variables.
2. Module mass is dependent upon standard mass of components utilized, say motor, gears, etc. and cannot be reduced below a limit.
3. For equivalent system, each module is sectioned into three prominent sections, leading to *APS-3*.

3.1. Equivalent system of point masses

Any rigid body that can be represented as distributed system of point masses provided the total mass, position of centre of mass (CoM) and inertia tensor of the rigid body is equal to the total mass, position of CoM and inertia tensor of the system of point masses, respectively, defined with respect to the same frame of reference.[23] Let the rigid body be represented by k number of the point masses m_j, $j \in 1:k$ and each having the coordinates with respect to a reference frame say, x, y & z. Equation (1) is used to equate the total mass of the rigid body with the distributed point masses, as

$$\sum_{j=1}^{k} m_j = m. \tag{1}$$

Location of the CoM is computed through

$$\sum_{j=1}^{k} m_j x_j = m\bar{x}; \sum_{j=1}^{k} m_j y_j = m\bar{y}; \sum_{j=1}^{k} m_j z_j = m\bar{z}. \tag{2}$$

Elements of inertia tensor of the rigid body are computed from point mass values and location coordinates as:

$$\begin{aligned} &\sum_{j=1}^{k} m_j\left(z_j^2 + y_j^2\right) = I_{xx}; \quad \sum_{j=1}^{k} m_j\left(x_j^2 + z_j^2\right) = I_{yy}; \\ &\sum_{j=1}^{k} m_j\left(x_j^2 + y_j^2\right) = I_{zz}; \quad \sum_{j=1}^{k} m_j x_j y_j = I_{xy}; \\ &\sum_{j=1}^{k} m_j y_j z_j = I_{yz}; \quad \sum_{j=1}^{k} m_j x_j z_j = I_{zx}. \end{aligned} \tag{3}$$

Equations (1), (2) and (3) together define equimomental conditions[23] that need to satisfy to represent a rigid body into point mass system and vice-versa.

3.2. Point mass model in a plane

For planar case, Eqs. (1), (2) and (3) reduce to only 4 in number, as

$$\sum_{j=1}^{k} m_j = m; \tag{4}$$

$$\sum_{j=1}^{k} m_j x_j = m\bar{x}; \sum_{j=1}^{k} m_j y_j = m\bar{y}; \tag{5}$$

$$\sum_{j=1}^{k} m_j\left(x_j^2 + y_j^2\right) = I_{zz}. \tag{6}$$

A single link is shown in Fig. 3. Equimomental three-point masses are shown through $X_1 - Y_1$ frame with origin O_1 for link 1. Equimomental equations are valid if both the systems that is point mass system and the rigid body are represented with respect to same $X_1 - Y_1$ frame. Positions of the

https://doi.org/10.1017/S0263574720001174 Published online by Cambridge University Press

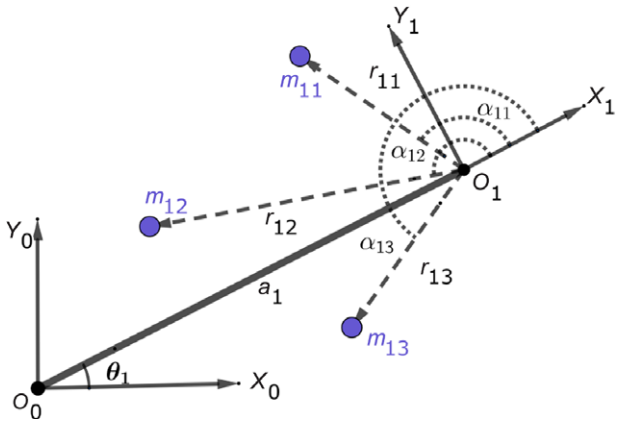

Fig. 3. Equimomental system using three-point mass system in planar links.

point masses are taken in terms of α_{ij} & r_{ij}, $j \in 1:3$ & $i \in 1:n$, where n is the number of DoF and links and thus would be $[r_{ij}\cos(\alpha_{ij}), r_{ij}\sin(\alpha_{ij})]$. This helps in posing the constraints systematically rather than in random X, Y coordinates.

3.3. Objective function for optimization

Objective is to minimize the torques of all joints of the manipulator by readjusting the represented point masses of the modules, when the end-effector of a given manipulator is moving on a certain path. To formulate the single objective function, the root mean square of the torques over the complete path has been taken.[24] Generally, Newtonian and Lagrangian formulation are used for the formulation of equation of motion. Here, we have used Euler–Lagrange formulation and the equation is written as[25]

$$\frac{d}{dt}\left[\frac{\partial \mathcal{L}}{\partial \dot{q}_i}\right] - \frac{\partial \mathcal{L}}{\partial q_i} = \tau_i, \tag{7}$$

where $i \in 1:n$, n is the number of DoF, $\mathcal{L}$ is the Lagrangian function which is equal to the difference of total kinetic energy (K) and total potential energy (P) of the system, q_i is the generalized coordinate for each joint and τ_i is the generalized force (or torque) applied to the system at the joint i to drive link i. Total kinetic and potential energy of a robot arm are

$$\begin{aligned} K &= \sum_{i=1}^{n} K_i = \frac{1}{2}\sum_{i=1}^{n} Tr\left[\sum_{p=1}^{i}\sum_{r=1}^{i} U_{ip} J_i U_{ir}^T \dot{q}_p \dot{q}_r\right], \\ P &= \sum_{i=1}^{n} P_i = -\sum_{i=1}^{n} m_i g\left({}^0A_i\, {}^i\bar{r}_i\right). \end{aligned} \tag{8}$$

where Tr is the trace operator, U_{ij} is the rate of change of the points $({}^i r_i)$ on link i relative to the base coordinate frame as q_j changes, J_i is the inertia of all the points in the link i, $J_i = \int {}^i r_i\, {}^i r_i^T dm$ and can be expressed as

$$J_i = \begin{bmatrix} \frac{-I_{xx}+I_{yy}+I_{zz}}{2} & I_{xy} & I_{xz} & m_i\bar{x}_i \\ I_{xy} & \frac{I_{xx}-I_{yy}+I_{zz}}{2} & I_{yz} & m_i\bar{y}_i \\ I_{xz} & I_{yz} & \frac{I_{xx}+I_{yy}-I_{zz}}{2} & m_i\bar{z}_i \\ m_i\bar{x}_i & m_i\bar{y}_i & m_i\bar{z}_i & m_i \end{bmatrix},$$

where m is the total mass of the link; $\bar{x}$, $\bar{y}$, $\bar{z}$ is the CoM and I_{xx}, I_{xy}, I_{xz}, I_{yy}, I_{yz}, I_{zz} are the elements of the inertia tensor of the link expressed in the i^{th} coordinate frame, $g = (g_x, g_y, g_z, 0)$ is a gravity

https://doi.org/10.1017/S0263574720001174 Published online by Cambridge University Press

row vector expressed in base coordinate and ${}^0A_i$ is the transformation matrix, representing frame $\{i\}$ with respect to the base frame $\{0\}$. Substituting Eq. (8) into (7) leads to equation of motion as

$$\tau(t) = D(\ddot{q}(t)) + h(q(t), \dot{q}(t)) + G(q(t)). \tag{9}$$

where $\tau(t) \in \Re^n$ is a vector of joint torques, $D(\ddot{q}(t)) \in \Re^{n\times n}$ is an inertial acceleration-related symmetric matrix, $h(q(t), \dot{q}(t)) \in \Re^n$ is a Coriolis and centrifugal force vector and $G(q(t)) \in \Re^n$ is gravity loading force vector. n is the number of DoF. Manipulator parameters of the modular assembly and sequence of the assembled modules are to be used as input and output is the generalized joint torques. The objective function is finally defined as weighted sum of root mean square of joint torques over the entire path.

$$f(x) = \sum_{i=1}^{n} w_i \tau_{(rms)_i}, \tag{10}$$

where $f(x)$ is the objective function. The weights (w_i) are given arbitrary according to the user requirement for each joint. Selection of weights is such that the summation $\sum_{i=1}^{n} w_i = w_1 + w_2 + \ldots w_n = 1$. The value of the weight to the respective joint torque can be given based on how much influence of that joint is required to be considered. As an example, for a 2-DoF system, for both equivalent joints, equal weights of 0.5 would be considered. For larger number of DoF, to keep the torque requirement less at farther joints, respective weight values should be high.

3.4. Optimization model

A link of a manipulator can be treated as a set of point masses placed at certain distances. The values of these point masses and their locations with respect to the frame of reference can be tuned to get the new CoM location and inertia tensor while considering our assumptions. Initially, for a given link, the three-point masses are considered by sectioning the three prominent elements of the module. All the point mass parameters as discussed in Section 3.2 are treated as design variables. Thus, optimization formulation for the above discussed problem can be posed as:

Design variables:

$$x = [m_{i1}, m_{i2}, m_{i3}, r_{i1}, r_{i2}, r_{i3}, \alpha_{i1}, \alpha_{i2}, \alpha_{i3}],\ for i = 1 : n. \tag{11}$$

To minimize:

$$f(x) = \sum_{i=1}^{n} w_i \tau_{(rms)_i}. \tag{12}$$

Subjected to:

$$\begin{aligned}
&M^i_{initial} \le M^i_{optimized} \le 2M^i_{initial},\\
&\text{where, } M^i = \sum_{j=1}^{3} m_{ij},\ i = 1 : n;\\
&0.5r^{ij}_{initial} \le r^{ij}_{optimized} \le L;\\
&90^\circ \le \alpha_{ij} \le 270^\circ;\\
&\delta I^i_{original} - I^i_{optimized} \le 0;\\
&CoM_{optimized} - \Delta L \le 0.
\end{aligned} \tag{13}$$

The total number of design variables will be nine times the number of DoF. The objective function is taken as the sum of the root mean squares of the respective joint torques over a path and is factorized with the weight function such that $\sum_{i=1}^{n} w_i = 1$. Constraints in Eq. (13) are applied such that mass of the link should not decrease below the limit but may increase and the values of point masses may increase or decrease. The positions of the point masses are not allowed to reach far and also are bounded to be within the dimensions of link length (L). δ and Δ are the user-controlled values for

https://doi.org/10.1017/S0263574720001174 Published online by Cambridge University Press

the constraints to adjust the parameters as required. δ is used to factorize the original inertia value of the original architecture to the new inertia value for the optimized architecture. This constraint ensures the value to be reduced from the previous as per δ factor and is always positive, whereas Δ is used to ensure that the CoM of the optimized architecture does not goes beyond the prescribed distance, which is the factor of link length, from the origin of the joint frame.

The formulation is general in nature and is applicable for any modular architecture which needs to be worked upon, for example, the frameworks shown in Fig. 2 through systematic sectioning.

3.5. Path/Trajectory selection

Optimizing module parameters for a single trajectory may not give sufficient results to conclude the module architecture. Therefore, it is important to consider exemplary trajectories. To perform that, three-primitive-paths are used in this work. Optimized architectural planning based on these three primitive paths is assumed to be effective for other required trajectories. The three paths are defined as follows.

Rectilinear path. For a linear path of the end-effector, the length of the path is decided by given initial conditions of position (p_i, p_f) and velocities (v_i, v_f). For which $L = ||p_f - p_i||$, and v_i and v_f are 0. In parametric form, linear path in Cartesian space can be written as

$$\begin{aligned} p(s) &= p_i + \frac{\sigma}{L}(p_f - p_i), \\ \dot{p}(s) &= \frac{(p_f - p_i)}{L}\dot{\sigma}, \\ \ddot{p}(s) &= \frac{(p_f - p_i)}{L}\ddot{\sigma}, \end{aligned} \tag{14}$$

where $\sigma \in [0, L]$ is the arc length. For trapezoidal motion

$$\sigma(t) = \begin{cases} \dfrac{a_{\max} t^2}{2}, & t \in [0, T_s] \\ v_{\max} t - \dfrac{v_{\max}^2}{2a_{\max}}, & t \in [T_s, T - T_s] \\ -\dfrac{a_{\max}(t-T)^2}{2} + v_{\max} T - \dfrac{v_{\max}^2}{a_{\max}}, & t \in [T - T_s, T] \end{cases} \tag{15}$$

where, $T_s = \dfrac{v_{\max}}{a_{\max}}$ and $T = \dfrac{L}{v_{\max}} + T_s$.

Circular path. A point P on a circle in a Cartesian space will satisfy the following equation:

$$P(t) = C + R\cos\left(\frac{2\pi t}{T}\right)U + R\sin\left(\frac{2\pi t}{T}\right)V \tag{16}$$

where $t \in 0 : T$, T : total time to cover the path. N is a unit normal vector for the plane of the circle, C is the centre of the circle and R is the radius of the circle. U is a unit vector from C towards a point on the circle such that $V = N \times U$. where $t \in 0 : T$, T : total time to cover the path.

Lemniscate path. The lemniscate path in 2D Cartesian space can be written as

$$\begin{aligned} x(t) &= x_0 + \frac{a\cos(t)}{\sin(t)^2 + 1}, \\ y(t) &= y_0 + \frac{a\cos(t)\sin(t)}{\sin(t)^2 + 1}. \end{aligned} \tag{17}$$

Another important aspect is related to the trajectory parameters. How can we define the sizes? Here, the parameters are proposed to be selected based upon the workspace of a particular manipulator. The location of task and scale of the path is within the workspace volume of the candidate configuration, considering the link lengths.

https://doi.org/10.1017/S0263574720001174 Published online by Cambridge University Press

Table I. Geometrical and inertial parameters of the modules.

Parameters	**Heavy(H)**	**Medium(M)**	**Light(L)**
l (m)	0.465	0.348	0.232
m (kg)	4.844	2.029	0.606
$\bar{x}$ (m)	0.261	0.197	0.130
$\bar{y}$ (m)	0.000	0.000	0.000
$\bar{z}$ (m)	0.002	0.001	0.001
I^c_{xx}	0.008	0.002	0.000
I^c_{xy}	0.000	0.000	0.000
I^c_{xz}	0.001	0.000	0.000
I^c_{yy}	0.099	0.023	0.003
I^c_{yz}	0.000	0.000	0.000
I^c_{zz}	0.096	0.022	0.003

All parameters are in SI units.

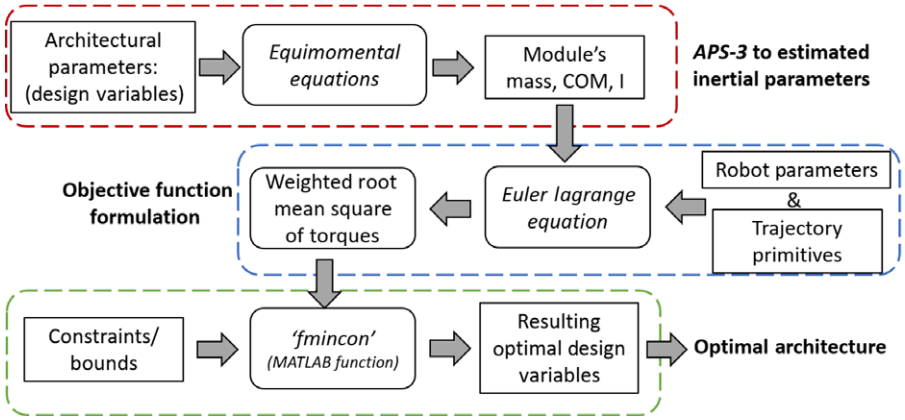

Fig. 4. Optimization process shown in three phases. First is the implementation of APS-3 and then estimating inertial parameters, second phase is the computation of the objective function and third phase is mapping of optimal results into a possible architecture.

3.6. Overall methodology structure: APS-3

The proposed methodology is shown in Fig. 4, where overall strategy is briefed. First phase consists of architecture sectioning and computing the rigid body parameters from the set of point mass parameters using equimomental Eqs. (1)–(3). In second phase, the computed rigid body parameters are fed to the Euler–Lagrange Eq. (9) along with manipulator parameters and trajectory, on which the end-effector has to run, to compute the torques and thus objective function. In the third phase, the *fmincon* function of *MATLAB optimization tool box* is used to solve the optimal design variables which will be mapped to realize architecture of a module.

4. Results

The strategy discussed above is implemented here for a modular configuration working in a plane which is composed of two number of modules. The modules for a reconfigurable manipulator are given as a set of three cascading sizes, heavy (H), medium (M) and light (L) as shown in Fig. 1(f), based upon the study conducted in ref. [2]. These modules are having similar architecture but differ in their sizes. The geometric and inertial parameters of the modules are mentioned in Table I. Modular configuration used here is composed of two number of modules as H and M. APS is done for both the modules and is shown in shown in Fig. 5. The equivalent point mass parameters that are fetched from the module elements are listed in Table II. As explained in Section 3.4, all the point mass parameters for this case are considered as design variables (11), objective function and constraints are used as Eqs. (12) and (13) in which following parameters are chosen as, $\delta = 0.5$ and $\Delta = 0.75$. The optimization problem is solved using *fmincon* function of *MATLAB optimization tool box* for all three paths as explained in Section 3.5.

https://doi.org/10.1017/S0263574720001174 Published online by Cambridge University Press

Table II. Point mass parameters of the modules after implementing APS-3.

Link	m_1	m_2	m_3	r_1	r_2	r_3	α_1	α_2	α_3
1	2.197	1.745	0.903	0.388	0.21	0.05	180	180	180
2	0.927	0.736	0.366	0.291	0.157	0.037	180	180	180

All parameters are in SI units.

Table III. Optimized point mass parameters of the modules for rectilinear path.

Path	**Link**	m_1	m_2	m_3	r_1	r_2	r_3	α_1	α_2	α_3
Linear	1	2.051	1.784	1.008	0.385	0.317	0.389	148.25	175.42	182.11
	2	0.896	0.788	0.343	0.348	0.348	0.018	132.931	186.52	185.75

Table IV. Optimized point mass parameters of the modules for circular path.

Path	**Link**	m_1	m_2	m_3	r_1	r_2	r_3	α_1	α_2	α_3
Circular	1	2.211	1.746	0.886	0.406	0.381	0.139	180.12	180.12	180.01
	2	1.015	0.728	0.285	0.291	0.280	0.14	139.36	157.34	176.16

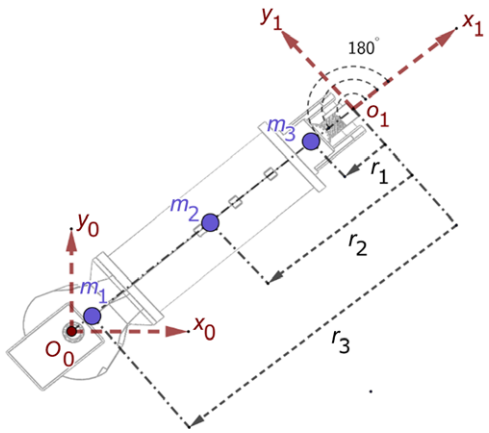

Fig. 5. Point mass representation of the module after implementing APS-3.

4.0.1. Rectilinear path. Using Eqs. (14) and (15) and substituting $v_{\max} = 0.2$; $a_{\max} = 0.1$; $p_i = [0.17, 0.17]$; $p_f = [0.60, 0.50]$, straight line will be formed as shown in Fig. 6. There has been 26.47% reduction in the objective function value as compared to the original parameters in this case. The re-adjusted point mass parameters are shown in Table III. Torque comparison plots are shown in Fig. 7(a) and (b) and is noticed that torque requirement for joint 1 is reduced but for joint 2, the torque has reduced at the start of trajectory but has increased in the mid and then again decreased to a certain level as compared to the initial torque where it has started with larger value and then decreases continuously. Changes in torque values are counteracting but overall function value has decreased significantly.

4.0.2. Circular path. Here, end-effector is allowed to follow the circular path as shown in Fig. 8 after substituting, $C = [0.3; 0.3; 0]$, $R = 0.1$, $N = [0; 0; 1]$, $U = [1; 0; 0]$ and $T = 5$ in Eq. (16). In this case, 22.6% reduction has been observed in the objective function value as compared to the original parameters. The re-adjusted point mass parameters are shown in Table IV. Torque comparison plots are shown in Fig. 9(a) and (b) and are noticed that torque requirement for joint 1 is reduced but for joint 2, the absolute value of the torques for the entire range has increased as compared to the initial torques. Changes in torque values in both joints are opposite, as it reduces in joint 1 and increases in joint 2, but the overall function value has decreased significantly in this case also.

https://doi.org/10.1017/S0263574720001174 Published online by Cambridge University Press

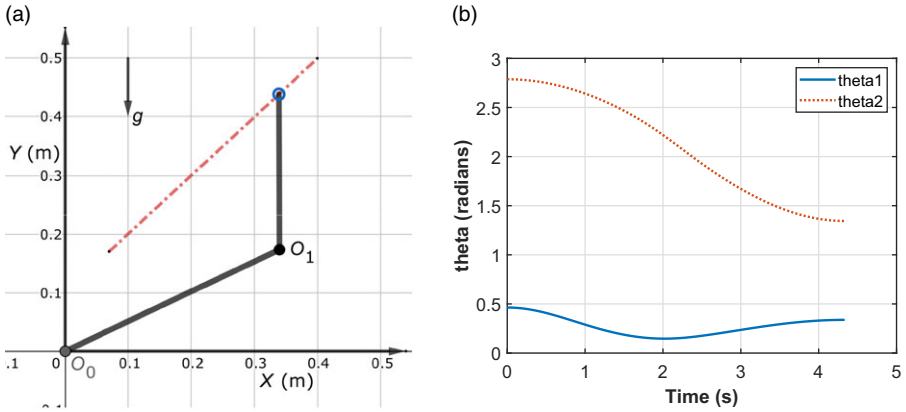

Fig. 6. (a) Rectilinear path for the end-effector in Cartesian space and (b) manipulator joint angles variation over the time T through inverse kinematics.

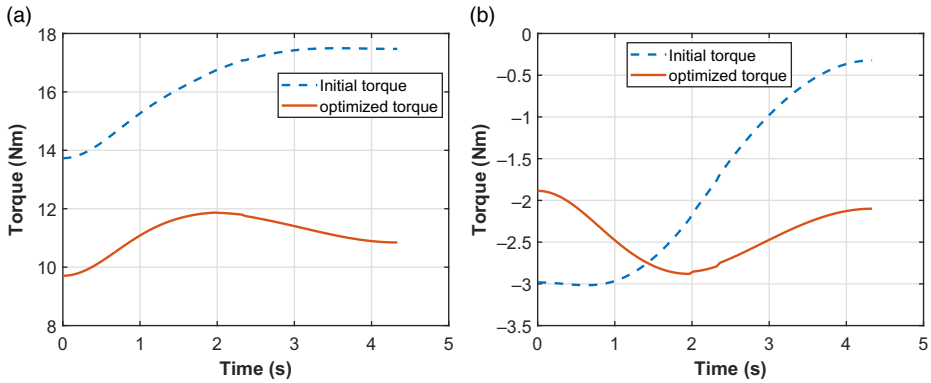

Fig. 7. Results of joint torque comparison between original and optimized links for rectilinear path: (a) torque comparison for rectilinear path in joint 1 and (b) torque comparison for rectilinear path in joint 2.

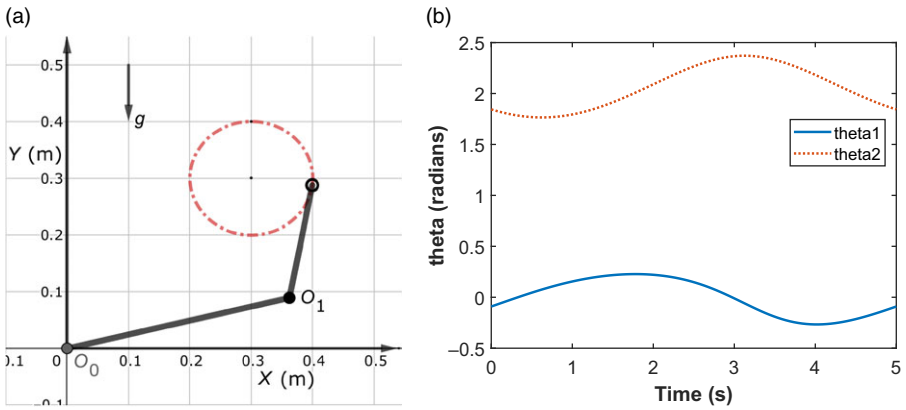

Fig. 8. (a) Circular path for the end-effector in Cartesian space and (b) Manipulator joint angles variation over the time T through inverse kinematics.

4.0.3. Lemniscate path. Here, substituting $x_0 = 0.2$, $y_0 = 0.4$, $a = 0.3\sqrt{2}$ and t in Eq. (17), where t varies from 0 to 7 s. Cartesian path and corresponding joint values for the manipulator are shown in Fig. 10. In this case, 29.79% reduction has been observed in the objective function value as compared to original parameters . The re-adjusted point mass parameters are shown in Table V. The torque comparison plots are shown in Fig. 11(a) and (b) and is observed that torque requirement for joint 1

https://doi.org/10.1017/S0263574720001174 Published online by Cambridge University Press

Table V. Optimized point mass parameters of the modules for lemniscate path.

Path	**Link**	m_1	m_2	m_3	r_1	r_2	r_3	α_1	α_2	α_3
Lemniscate	1	2.027	1.806	1.010	0.382	0.360	0.324	148.25	178.08	182.22
	2	0.854	0.783	0.391	0.252	0.281	0.289	139.48	165.12	178.098

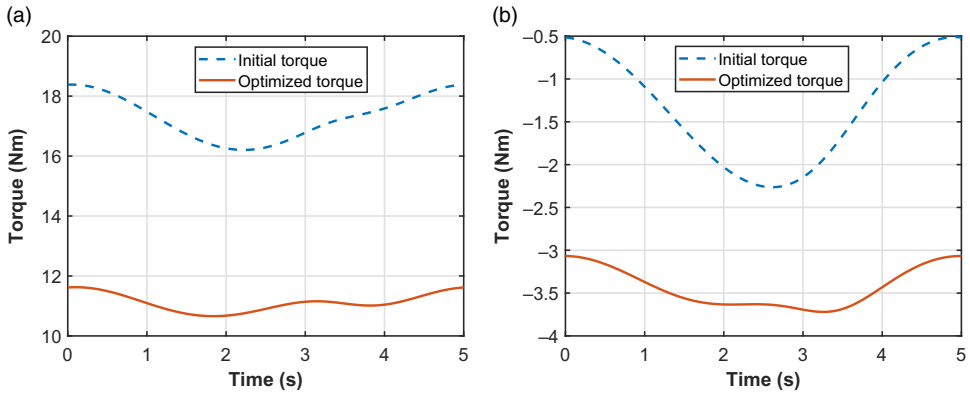

Fig. 9. Results of joint torque comparison between original and optimized links for circular path: (a) torque comparison for circular path in joint 1 and (b) torque comparison for circular path in joint 2.

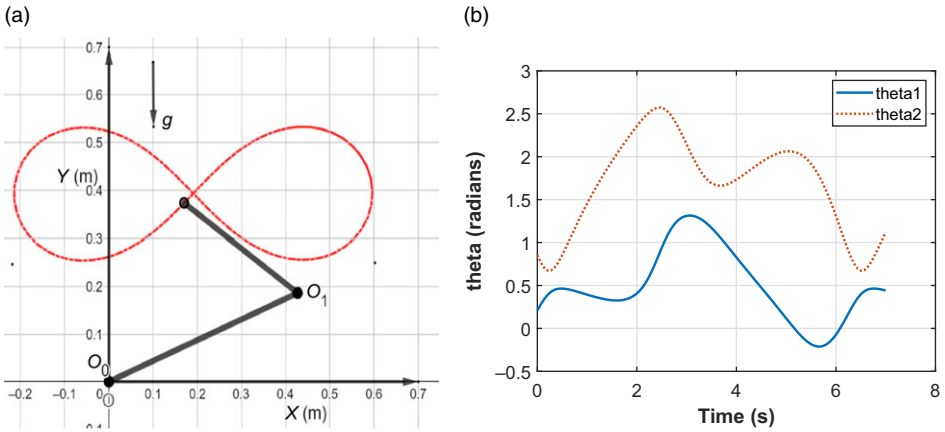

Fig. 10. (a) Lemniscate path for the end-effector in Cartesian space and (b) manipulator joint angles variation over the time T through inverse kinematics.

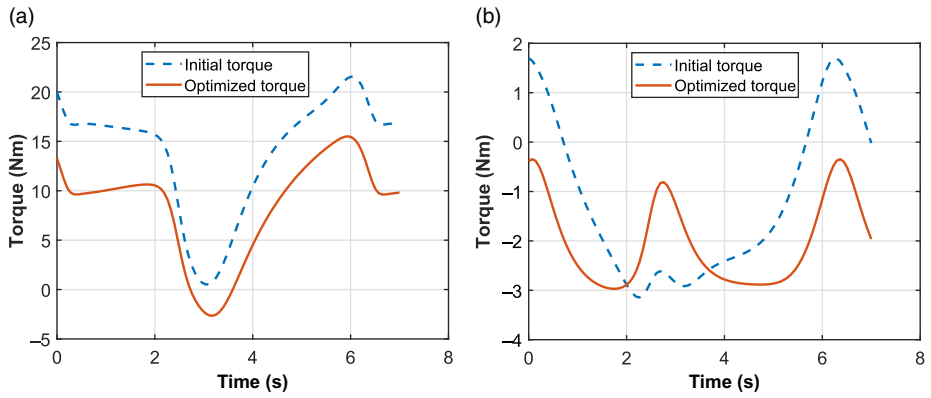

Fig. 11. Results of joint torque comparison between original and optimized links for lemniscate path: (a) torque comparison for lemniscate path in joint 1 and (b) torque comparison for lemniscate path in joint 2.

https://doi.org/10.1017/S0263574720001174 Published online by Cambridge University Press

Table VI. Optimized rigid body parameters of the modules.

Path	**Link(i)**	M_i	d_i	ϕ_i	I_c^i
Linear	1	4.844	0.348	164.67	0.048
	2	2.029	0.260	158.20	0.066
Circular	1	4.844	0.348	−179.88	0.048
	2	2.029	0.261	148.81	0.011
Lemniscate	1	4.844	0.348	165.71	0.048
	2	2.029	0.261	157.74	0.011

All parameters are in SI units.

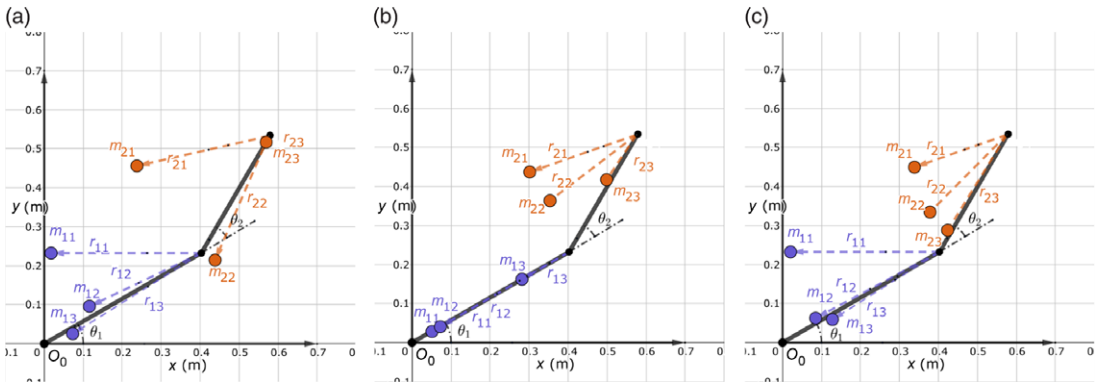

Fig. 12. Optimized point mass parameters for three cases. (a) Optimized point masses in case of linear path, (b) optimized point masses in case of circular path and (c) optimized point masses in case of lemniscate path.

is reduced a bit and also for joint 2, the torque for the entire range has decreased except in the middle, where it has decreased further as compared to the initial torque.

The results of optimization are different for the three cases discussed above. The torque requirement for each path has been reduced as the inertial parameters of the manipulator have been re-adjusted for both the modules. Optimized parameters of the modules for all three cases are shown in Table VI. In which M_i is the total mass of the module or link, d_i is the position of the CoM of the link i, ϕ_i is the angle between the axis along the link i and the CoM of the same link measured counter-clockwise and I_c^i is inertia of the link i with respect to the CoM. It can be observed from the results that the total mass of the modules has remained unchanged, whereas the magnitude of the CoM ($[\bar{x}, \bar{y}, \bar{z}]^T$) has come closer to the joints. Inertia about the CoM (I_c) has changed as per the constraints except in link 2 in the case of rectilinear path in which inertia has increased. The point masses have been re-adjusted at different locations and corresponding point mass visualization for all three cases can be seen in Fig. 12(a)–(c).

The key observation in the resulting optimized mass parameters as can be seen in Fig. 12(a)–(c) is that the optimized mass parameters are arranged nearer to each other. Such results may occur due to the range of radial constraints given in Eq. (13). For these results, one to one mapping of the point masses into an architecture becomes tedious.

To tackle this condition, the re-definition of the constraints has been done here, that is, the distances of point mass have to be varied in locality rather than in the complete domain as, $0.5r_{ij} \leq r_{ij} \leq 1.5r_{ij} \leq L$. It is worth noting that point masses are again re-adjusted with respects to new constraints without any change in function value of the objective function, rigid body parameters and torque plots. New parameters can be seen in Table VII and are shown in Fig. 13(a)–(c). Re-adjusted architecture of a module according to the optimized results by mapping the point masses into a complete architecture, taking three point masses as CoMs for each of the three sections, is shown in Fig. 14(a). The commonality between the location of the three point masses considering three cases is chosen to be the mapped point masses into the three prominent sections of the architecture.

https://doi.org/10.1017/S0263574720001174 Published online by Cambridge University Press

Table VII. Optimized point mass parameters of the modules with regional constraints.

Path	**Link(i)**	m_1	m_2	m_3	r_1	r_2	r_3	α_1	α_2	α_3
Linear	1	2.809	1.85	0.183	0.41	0.296	0.025	170.50	152.44	173.27
	2	1.169	0.81	0.049	0.348	0.235	0.018	176.64	116.67	174.52
Circular	1	2.605	1.817	0.421	0.420	0.310	0.073	180.54	179.62	180.24
	2	0.654	1.3742	0	0.348	0.235	0.044	169.68	137.24	175.32
Leminiscate	1	2.619	1.842	0.382	0.415	0.315	0.075	169.68	158.09	173.98
	2	1.071	0.957	0	0.299	0.235	0.0549	169.681	140.769	173.849

All parameters are in SI units.

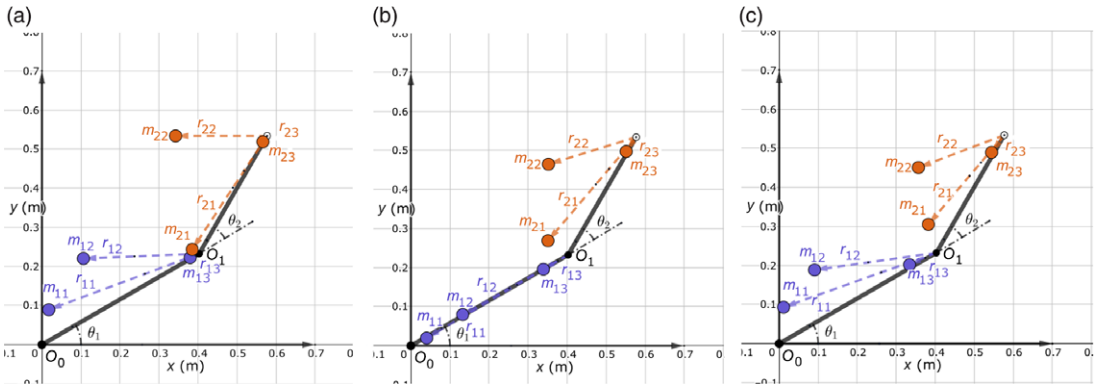

Fig. 13. Optimized point mass parameters for three cases for improved constraints. (a) Optimized point masses in case of linear path, (b) optimized point masses in case of circular path, (c) optimized point masses in case of lemniscate path.

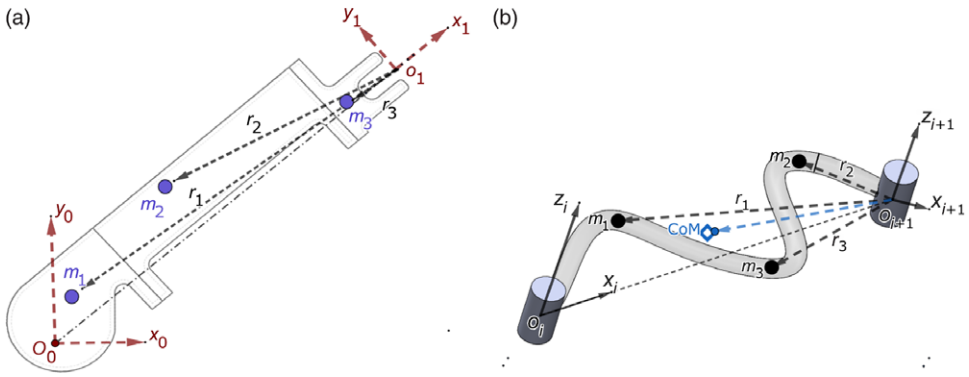

Fig. 14. Mapping of the point masses into architecture. (a) Optimized architecture of module and (b) possible optimal curved link.

5. Discussions

The *APS* implemented above for a modular configuration shows that there is a significant reduction in torque values and objective function when the mass parameters are re-adjusted even if the total mass remains the same, due to the re-position of the CoM and inertia terms. It is also observed that varying the constraints and bounds on the design variables within the limit causes negligible or no change in the objective function value and torque requirements, but point mass parameters are different in each case. This observation points out to have multiple solutions for each task, depending upon the constraints, bounds, start point, a user chooses. This gives the flexibility of getting desired point mass parameters based upon users criterion, keeping in mind the manufacturability of the shape. This *APS* strategy is proposed to be implemented on any kind of module or during the planning phase of designing a module architecture.

https://doi.org/10.1017/S0263574720001174 Published online by Cambridge University Press

Synthesizing a shape from the given rigid body parameters is not straight forward but one can use the optimized point masses to approximate the shape. Rather than solving a topological problem for a rigid link, one can approximate the link architecture by directly mapping the optimized equimomental system or the point masses into a new architectural design. Redistribution of point masses is planned through redefining the component locations and alterations in modular component selection, say actuator or gear-box orientation and location, if required.[26] One option is to focus on the material characteristics for printing the modular sections based on the optimal results, using upcoming advanced technologies in additive manufacturing field. In multi-body systems, kinematics only cares about the position and orientation of the two frames at the two ends of the link. So to give a general orientation to the distal frame of the link with respect to the proximal frame, any curved shape link can be used which fulfills the purpose. The issue is to consider the effect of dynamic performance. The idea of this work also tends towards to give an optimal shape of the link or configuration of the general/curved links.[27] The general link configuration can be approximated by directly mapping the set of point mass parameters as shown in Fig. 14(b). It is a bit difficult to attain exact results for the general shaped rigid body to match with the point mass system but still, a nearly optimal solution can be achieved which will result in reduced torques for the joints. The configured shape may assume to interpolate or approximate the locations of the point masses. The values of total mass and the CoM could be satisfied, but challenges remain in matching its inertia tensor and that needs to be addressed in our future works. The exact analysis of synthesizing these shapes is not given here in this work, but an idea of approximating the general shapes has been tried. The curved swept profile can have uniform density all over or further optimization problems for the cross-sectional profile can be formulated to give the best near-optimal results equivalent to point mass models.

6. Conclusion

An idea of planning an optimal architecture of a module, based upon dynamic performance, is presented. First, a given module is represented as a set of equivalent point masses, assumed as sections of the modules, according to *APS* strategy and then, an optimization formulation is done to optimize the point masses and their positions for which objective function is chosen as minimizing the joint-torques. The optimization formulation is simulated on a modular configuration whose end-effector has to follow a given trajectory. The optimized point mass parameters are used as it is to re-map into a rigid body as to approximate a new architecture. An idea of getting the advance/complex shapes of the modules is also discussed, for which strategy is to be developed in future works.

References

1. H. Ahmadzadeh, E. Masehian and M. Asadpour, "Modular robotic systems: Characteristics and applications," *J. Intell. Rob. Syst.* **81**(3–4), 317–357 (2016).
2. S. Singh, A. Singla and E. Singla, "Modular manipulators for cluttered environments: A task-based configuration design approach," *J. Mech. Rob.* **10**(5), 051010 (2018).
3. J. A. Kereluk and M. R. Emami, "Task-based optimization of reconfigurable robot manipulators," *Adv. Rob.* **31**(16), 836–850 (2017).
4. N. Stravopodis, C. Valsamos and V. C. Moulianitis, "An Integrated Taxonomy and Critical Review of Module Designs for Serial Reconfigurable Manipulators," *Proceedings of International Conference on Robotics in Alpe-Adria Danube Region* (2019) pp. 3–11.
5. S. Singh and E. Singla, "Realization of task-based designs involving DH parameters: A modular approach," *Intell. Serv. Robot.* **9**(3), 289–296 (2016).
6. J. Liu, X. Zhang and G. Hao, "Survey on research and development of reconfigurable modular robots," *Adv. Mech. Eng.* **8**(8), 1687814016659597 (2016).
7. E. Icer, H. A. Hassan, K. El-Ayat and M. Althoff, "Evolutionary Cost-Optimal Composition Synthesis of Modular Robots Considering a Given Task," *Proceedings of IEEE/RSJ International Conference on Intelligent Robots and Systems (IROS)* (2017) pp. 3562–3568.
8. T. Campos, J. P. Inala, A. Solar-Lezama and H. Kress-Gazit, "Task-Based Design of Ad-hoc Modular Manipulators," *Proceedings of IEEE International Conference on Robotics and Automation (ICRA)* (2019) pp. 6058–6064.
9. H. Seonghun, C. Dongeun, K. Sungchul, H. Lee and W. Lee, "Design of Manually Reconfigurable Modular Manipulator with Three Revolute Joints and Links," *Proceedings of IEEE International Conference on Robotics and Automation (ICRA)* (2016) pp. 5210–5215.
10. G. Acaccia, L. Bruzzone and R. Razzoli, "A modular robotic system for industrial applications," *Assembly Autom.* **28**(2), 151–162 (2008).
11. M. Brandstoetter, Adaptable Serial Manipulators in Modular Design *Doctoral Dissertation, Ph.D. Thesis, UMIT* (2016).

https://doi.org/10.1017/S0263574720001174 Published online by Cambridge University Press

12. V. C. Moulianitis, A. I. Synodinos, C. D. Valsamos and N. A. Aspragathos, "Task-based optimal design of metamorphic service manipulators," *J. Mech. Rob.* **8**(6), 061011 (2016).
13. S. Patel and T. Sobh, "Manipulator performance measures-a comprehensive literature survey," *J. Intell. Rob. Syst.* **77**(3–4), 547–570 (2015).
14. O. Chocron, "Evolutionary design of modular robotic arms," *Robotica* **26**(3), 323–330 (2008).
15. W. A. Khan and J. Angeles, "The kinetostatic optimization of robotic manipulators: The inverse and the direct problems," *J. Mech. Des.* **128**(1), 168–178 (2006).
16. R. P. Mohamed, F. J. Xi and A. D. Finistauri "Module-based static structural design of a modular reconfigurable robot," *J. Mech. Des.* **132**(1), 014501 (2010).
17. D. Ramirez, J. Kotlarski and T. Ortmaier, "Combined Structural-Dimensional Synthesis of Robot Manipulators for Minimal Energy Consumption," *Proceedings of Tagungsband des 2. Kongresses Montage Handhabung Industrieroboter* (2017) pp. 63–71.
18. B. Wei and D. Zhang, "A review of dynamic balancing for robotic mechanisms," *Robotica*, 1–17 (2020).
19. V. Arakelian, J.-P. Le Baron and P. Mottu, "Torque minimisation of the 2-DOF serial manipulators based on minimum energy consideration and optimum mass redistribution," *Mechatronics* **21**(1), 310–314 (2011).
20. K. Chaudhary and H. Chaudhary, "Optimal dynamic balancing and shape synthesis of links in planar mechanisms," *Mech. Mach. Theory* **93**, 127–146 (2015).
21. L. Zhou and S. Bai, "A new approach to design of a lightweight anthropomorphic arm for service applications," *J. Mech. Robot.* **7**(3), 031001 (2015).
22. A. Dogra, S. S. Padhee and E. Singla "Towards Dynamics and Control of Modular Reconfigurable Manipulators," *Proceedings of the Advances in Robotics (AIR)* (2019) pp. 1–6.
23. H. Chaudhary and S. K. Saha, *Dynamics and Balancing of Multibody Systems* (1st ed., Vol. 37, Springer-Verlag, Berlin, Heidelberg, 2009).
24. V. Gupta, S. K. Saha and H. Chaudhary, "Optimum design of serial robots," *J. Mech. Des.* **141**(8), 082303 (2019).
25. K. S. Fu, R. Gonzalez and C. G. Lee, *Robotics: Control Sensing. Vis.* (Tata McGraw-Hill Education, New Delhi, India, 1987).
26. A. Dogra, S. S. Padhee and E. Singla, "An optimal architectural design for unconventional modular reconfigurable manipulation system," *ASME. J. Mech. Des.* **143**(6), 063303 (2020).
27. M. Brandstötter, P. Gallina, S. Seriani and M. Hofbaur, "Task-Dependent Structural Modifications on Reconfigurable General Serial Manipulators," *Proceedings of International Conference on Robotics in Alpe-Adria Danube Region* (2018) pp. 316–324.

https://doi.org/10.1017/S0263574720001174 Published online by Cambridge University Press